Self-Assembled Monolayers

International Edition: DOI: 10.1002/anie.201906247
German Edition: DOI: 10.1002/ange.201906247

On-Surface Reactive Planarization of Pt(II) Complexes

Jindong Ren, Marvin Cnudde, Dana Brünink, Stefan Buss, Constantin G. Daniliuc, Lacheng Liu, Harald Fuchs, Cristian A. Strassert, Hong-Ying Gao,* and Nikos L. Doltsinis**

Abstract: *A series of Pt(II) complexes with tetradentate luminophores has been designed, synthesized, and deposited on coinage metal surfaces with the aim to produce highly planar self-assembled monolayers. Low-temperature scanning tunneling microscopy (STM) and density functional theory (DFT) calculations reveal a significant initial nonplanarity for all complexes. A subsequent metal-catalyzed separation of the nonplanar moiety at the bridging unit via the scission of a C–N bond is observed, leaving behind a largely planar core complex. The activation barrier of this bond scission process is found to depend strongly on the chemical nature of both bridging group and coordination plane, and to increase from Cu(111) through Ag(111) to Au(111).*

Electroluminescent emitters based on transition metal complexes have gained much attention due to their applications in organic light-emitting diodes for display and lighting technologies.[1,2] Pt(II) complexes display both high quantum efficiencies and low quenching effects as a consequence of the large spin-orbit coupling.[3,4] They exhibit a mostly square-planar coordination due to their d^8 electronic configuration, making them ideal candidates to achieve ordered layered structures. Furthermore, molecular stacking causes the doubly occupied d_{z^2} orbitals to split into a σ-type bonding and antibonding pair of intermetallic orbitals, red-shifting the emitted wavelengths and influencing the photoluminescence quantum yields.[5,16] Thus, it is desirable to synthesize Pt(II) complexes with planar ligands as they would enable the controlled fabrication of electroluminescent devices consisting of multilayered arrays.[6] While much progress has been made recently on the molecular design of individual Pt(II) complexes with desired properties by a combination of chemical knowledge and quantum-chemical calculations, their interactions with metal substrates are still difficult to predict. In addition to altering the physical properties of molecular adsorbates, metal surfaces are known to enable a plethora of chemical reactions,[7–9] which have, for instance, been exploited to build novel nanostructures.[10,11] Hence, it may also be possible to apply this substrate-catalyzed reaction approach[12,13] to the on-surface chemical modification of Pt(II) complexes, circumventing potential difficulties in traditional wet-chemical synthesis to controllably obtain tailored Pt(II) complexes.

Here we report the unexpected surface-mediated scission of a C–N bond in a series of organometallic Pt(II) complexes with tetradentate luminophores. To examine what factors influence the C–N bond scission, the precursor Pt(II) complexes were prepared with different moieties at the bridging N-atoms (see Scheme 1) in solution by straightforward synthesis[14] and then sublimed onto three different metal surfaces (Au(111), Ag(111), and Cu(111)) under ultrahigh-vacuum conditions[15] (see the Supporting Information for experimental details and spectroscopic characterization). This series of experiments aims to shed light on the influence of the

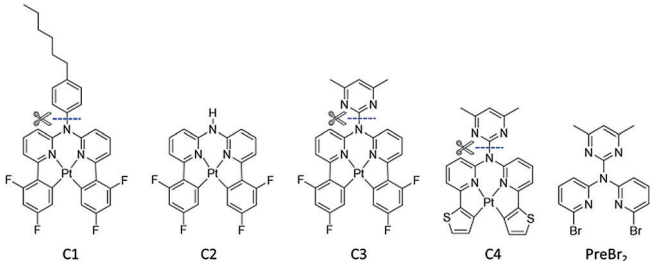

Scheme 1. Chemical structures of complexes **C1**–**C4** and **PreBr$_2$**.

[*] Dr. J. Ren, L. Liu, Prof. Dr. H. Fuchs, Dr. H.-Y. Gao
Physikalisches Institut, Westfälische Wilhelms-Universität Münster
Wilhelm-Klemm-Straße 10, 48149, Münster (Germany)
E-mail: gaoh@uni-muenster.de

M. Cnudde, S. Buss, Prof. Dr. C. A. Strassert
Institut für Anorganische und Analytische Chemie
Westfälische Wilhelms-Universität Münster
Corrensstraße 28/30, 48149 Münster (Germany)
E-mail: cstra_01@uni-muenster.de

Dr. J. Ren, M. Cnudde, S. Buss, L. Liu, Prof. Dr. H. Fuchs, Prof. Dr. C. A. Strassert, Dr. H.-Y. Gao
Center for Nanotechnology (CeNTech)
Heisenbergstrasse 11, 48149, Münster (Germany)

D. Brünink, Prof. Dr. N. L. Doltsinis
Institut für Festkörpertheorie and Center for Multiscale Theory and Computation, Westfälische Wilhelms-Universität Münster
Wilhelm-Klemm-Straße 10, 48149 Münster (Germany)
E-mail: nikos.doltsinis@uni-muenster.de

Dr. C. G. Daniliuc
Organisch-Chemisches Institut
Westfälische Wilhelms-Universität Münster
Corrensstraße 40, 48149 Münster (Germany)

Dr. H.-Y. Gao
School of Chemical Engineering and Technology, Tianjin University
Tianjin 300072 (China)

Supporting information and the ORCID identification number(s) for the author(s) of this article can be found under: https://doi.org/10.1002/anie.201906247.

chemical composition and geometry of the Pt(II) complexes and the nature of the substrate on the C–N bond scission. For a coplanar coordination plane and bridging group, the interaction with the substrate is expected to be maximized, enhancing C–N bond cleavage compared with the case where the core and bridging moiety are perpendicular to each other. In particular, it is intuitively clear that the closer the C–N bond is to the surface, the easier its activation should become.

Of the synthesized complexes shown in Scheme 1, **C3** and **C4** are expected to have stronger interactions with the substrate than complex **C1**. This is because steric hindrance forces the phenyl bridging group of **C1** to be orthogonal to the coordination plane, while the pyrimidine unit of **C3** and **C4** should, in principle, favor a more coplanar arrangement. Owing to its sulfur atoms,[16] the core ligand of **C4** should interact more strongly with the substrate than that of **C3**. Our goal is to study what consequences the geometric differences between **C1**, **C3**, and **C4** have for C–N bond activation.

Initially, complex **C1** was chosen because of its favorable phosphorescence properties.[14] Figure 1 a-1 depicts the large-scale STM topography of a Cu(111) surface covered by one-dimensional chains after thermally evaporating **C1**. All STM images below were acquired with a tunneling current of $I = -0.03$ nA and a voltage of $V_b = -0.20$ V. Details of the molecular configuration in each chain can be found in the high-resolution image (Figure 1 a-2) and the corresponding molecular model (Figure 1 a-3), which fits the topographic image well. No fragmented molecules are visible on the surface. We therefore conclude that the molecules are intact after sublimation from the heated source and predominantly form head-to-tail dimers. The bright spots of **C1** in the STM image are assigned to the phenyl rings, which are connected to each other by van der Waals interactions to form self-assembled chains.[17] The fact that the phenyl ring appears brighter than both the central Pt atom and the tetradentate core ligand indicates that the phenyl ring is not oriented parallel to the substrate, but stands nearly perpendicular to the surface.

To investigate possible surface-mediated reactions, we annealed the sample gradually (see Figure 1 b,c and Figure S60 b). After the temperature had been raised to 405 K for 10 min, many dimers adopted a more elongated head-to-tail structure in which the alkane chains are arranged parallel to each other.[14] The Pt–Pt distance within the dimer increases from 1.84 ± 0.07 nm to 2.42 ± 0.08 nm. Intact monomers can also be clearly identified, with a bright phenyl bridge feature and a central bright dot corresponding to the protruding d_{z^2} orbital of the Pt center.[14]

Subsequently, the sample was annealed to 435 K for 10 min. Some "clover-like" moieties started to be observed (see Figure S60 b), which were identified as complex **C2**, resulting from a C–N scission reaction in **C1**, and the yield of **C2** was seen to increase further after annealing the sample above 475 K (Figure 1 c).

For comparison and verification of our above interpretation, complex **C2** was directly synthesized. We stress, however, that this was not straightforward, largely due to the low solubility of **C2**. The complexes were then deposited on Cu(111) at room temperature, leading to disperse adsorbate STM features (see Figure 2 a) similar to those of Figure 1 c.

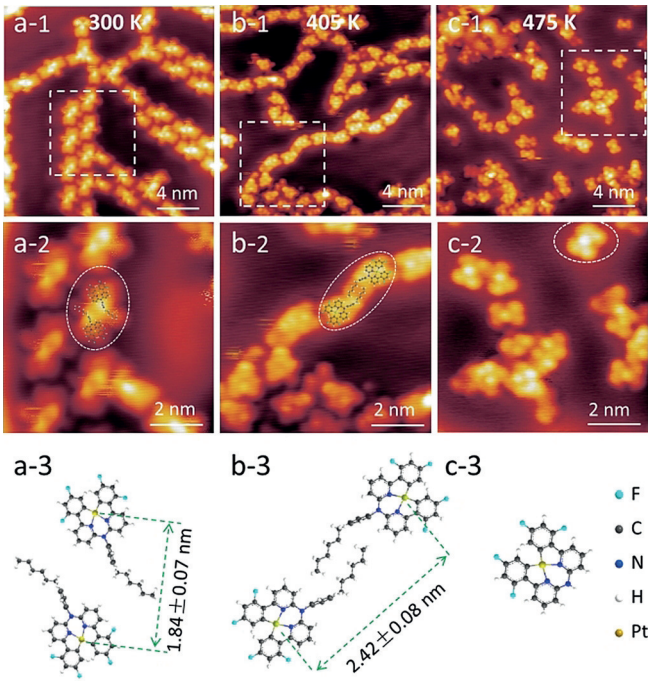

Figure 1. Top row: STM topographies of complex C1 on Cu(111) surface at different annealing temperatures. Middle row: Close-ups of selected areas of the images above. Bottom row: Interpretations of the highlighted areas of the STM images in the middle row in terms of molecular models.

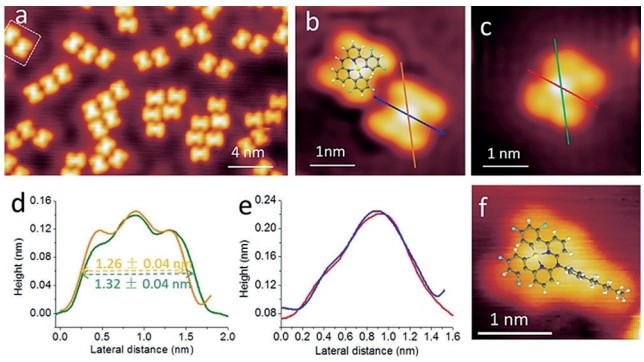

Figure 2. a,b) STM topographies of the reference complex **C2** on Cu(111). c) Close-up image of moiety highlighted in Figure 1 c-2 after annealing **C1** on Cu(111). d,e) Line profiles along different directions defined in (b) and (c). f) Close-up image of **C1** on Cu(111) before annealing with molecular structure superimposed.

The close-up STM images of **C2** and annealed **C1** (Figures 2 b,c) show a strong similarity. Both, in turn, are markedly different from the close-up image of **C1** before annealing (Figure 2 f), in which the bridging group can clearly be seen. The superimposed molecular structure of **C2** fits its STM image well (Figure 2 b). Line profiles along different directions further show that both molecules have the same size (Figure 2 d,e), the diagonal of the "clover-like" features measuring 1.26 ± 0.04 nm and 1.32 ± 0.04 nm, respectively.

Furthermore, both profiles exhibit a small shoulder around 0.4 nm from the center (Figure 2e), pointing at the existence of an N atom.

In the case of the annealing product of **C1**, the cleaved C–N bond is likely to be saturated by hydrogens, which might be transferred from the leaving bridging group[18] or from H_2 molecules present in the vacuum[19] as previously reported. In our STM images no additional fragments were found on the surface, indicating desorption of the cleaved bridging groups.

The proposed catalytic fragmentation was further investigated by DFT calculations (for technical details see the Supporting Information) of complex **C1** (without the alkyl chain) on Cu(111). Using constrained optimization along the C–N coordinate, the reaction mechanism and the corresponding energy profile were computed (Figure 3). A barrier of

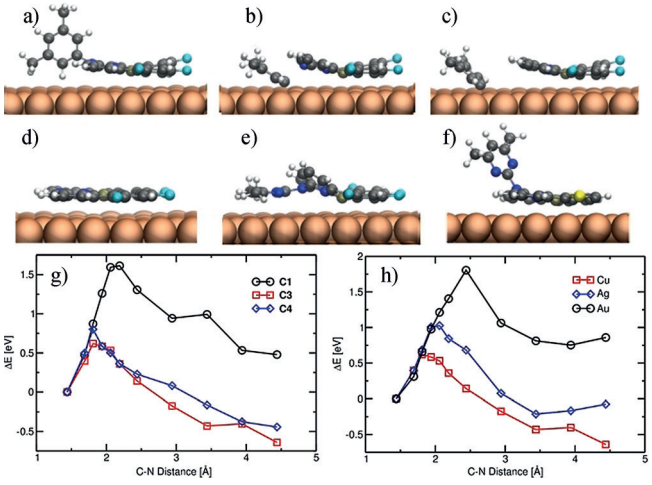

Figure 3. Top row: Constraint-optimized structures of a **C1** analogue (without the alkyl chain, but two methyl groups in *meta* position to speed up the calculations) on Cu(111) along the C–N dissociation path at a C–N bond length of 1.4 Å (optimized value) (a), 2.2 Å (b), and 4.4 Å (c). Second row: Optimized structures of **C2** (d), **C3** (e), **C4** (f) on Cu(111). Bottom row: Energy profiles for C–N scission of **C1**, **C3**, and **C4** on Cu(111) (g) and of **C3** on Cu(111), Ag(111), and Au(111) (h).

1.7 eV is reached at a C–N distance of 2.2 Å, confirming that high temperatures are required for this reaction to occur. Once the C–N bond is broken, the C atom covalently binds to the metal (Figure 3b), such that the bridging group eventually assumes an orientation almost perpendicular to the surface (Figure 3c). During the reaction, the top-layer Cu atoms in the vicinity of the severed C–N bond are strongly displaced. At a separation of 3.4 Å, the Cu atom in between the C and N atoms is lifted 0.46 Å above the surface, suggesting that extraction of metal atoms is a possibility at mild temperature.[20] Indeed, at the high annealing temperatures necessary to trigger C–N scission, large amounts of cluster by-products were also observed in the STM pictures which were previously ascribed to C–H activation.[21]

To improve the reaction efficiency and obtain higher purity products,[22] we next designed and investigated similar precursors, however, with more favorable geometries. A particular design goal was to change the orientation of the moiety at the bridge from perpendicular to the surface (as in **C1**) to coplanar, as such an arrangement maximizes the catalytic interaction between the metal and the adsorbate. Therefore, we replaced the phenyl bridging group by a pyrimidine ring (complex **C3**), eliminating the steric hindrance caused by the phenyl hydrogens, which led to the perpendicular orientation with respect to the core ligand and thereby to the surface.

Complex **C3** was deposited on Cu(111) for 5 min at 300 K before the sample was cooled down to 78 K. On the STM image (Figure 4) around 80% of all complexes were identified to be intact, while the rest show the same topography as in Figure 2c, meaning that C–N bond scission has already taken place at room temperature in this case. Moreover,

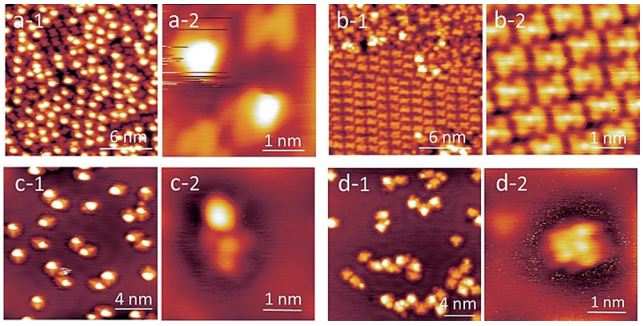

Figure 4. STM topographies of complex **C3** (a,b) and **C4** (c,d) on Cu(111) before (a,c) and after (b,d) annealing at 385 K.

keeping the sample at 300 K for 5 h or annealing the sample to 385 K for 5 min, resulted in the transformation of nearly all of the complexes to product **C2** (Figure 4b).

Our DFT calculations also confirm that **C3** has an almost fully planar structure on Cu(111) in contrast to **C1** (see Figure 3a,e) and a drastically reduced activation barrier of 0.62 eV (Figure 3g). It is plausible to infer that, because complex **C3** is overall closer to the surface, the fragmentation reaction is accelerated compared to complex **C1**. Moreover, the mild reaction conditions also prevented any unwanted by-products (Figure S60b).

To further develop and test the concept of tuning C–N scission by precursor geometry, we additionally designed complex **C4**, whose main ligand features two thiophene rings instead of two phenyl rings as in **C1** and **C3**, and repeated the above experiments. This modification is expected to enhance the interactions between the coordination plane and the substrate at the position of the sulfur atoms, which may have a noticeable effect on C–N scission.

Figure 4c-1 and 4c-2 show the STM images of the Cu(111) surface covered by a submonolayer of **C4**. Due to the strong interaction between the thiophene group and the Cu surface, pulling the core ligand down on one end, the other end of the coordination plane is seen to protrude into the vacuum (Figure 4c-2), which means the C–N bond is slightly lifted off the surface. This would explain the fact that fragmentation was not observed at room temperature. However, when the sample was annealed at 385 K, C–N fragmentation clearly

started to take place, albeit with lower efficiency as compared to **C3**. Apart from intact **C4** complexes, products without bright protrusion could also be found on the surface (Figure 4d-1 and 4d-2).

It is important to note that attempts to produce the reaction product of **C4** (i.e. the thiophenyl analogue of **C2**) by direct synthesis were unsuccessful, mainly due to purification issues. However, the STM findings are corroborated by our DFT calculations, which yield a slightly higher activation barrier of 0.80 eV for **C4** than for **C3**. This is firstly due to the fact that, in this case, an armchair-shaped conformer with a protruding group at the bridging N (Figure 3f) is marginally more stable by 0.12 eV than the flat-bridge conformer, which is similar to the most stable **C3** conformer shown in Figure 3e. However, since the armchair conformer is unreactive, the reaction proceeds via the flat-bridge conformer. Its optimized geometry reveals that one of the two S atoms binds very strongly to the metal surface (the shortest S–Cu distance being 2.7 Å), while the other stands out much further (3.3 Å to the nearest Cu atom). Crucially, compared to **C3**, the C atom of the reactive C–N bond in **C4** is on average 0.05 Å further away from each of the nearest three Cu atoms of the hollow site it occupies. The results therefore suggest that there is a correlation between the C–Cu distance and the activation barrier.

In summary, the order **C3** > **C4** > **C1** in terms of reactivity is observed experimentally, which is in good agreement with the theoretical activation barriers (Figure 3g). We have verified that this trend and the proposed reaction mechanism are true for other coinage metal surfaces by repeating the studies on Ag(111) and Au(111), albeit with increased activation barriers (Figure 3h). We could indeed confirm by STM imaging that the scission reaction also occurs on Ag(111), but at elevated annealing temperatures of 455 K, 390 K, and 410 K for **C1**, **C3**, and **C4**, respectively (Figure S62). On Au(111), no fragmentation was observed for **C1**, **C3**, or **C4**. Instead, the intact complexes were seen to form large aggregates after annealing (Figure S61).

Since the C–N scission reaction occurs for a number of Pt complexes with different ligands, it is important to point out that the Pt atom appears to play an essential role in the core-planar system, triggering the catalytic activity of the substrate. This was confirmed in control experiments with the ligand precursor **PreBr$_2$** (Scheme 1), which does not contain a Pt center, where no fragmentation at the C–N position was observed (Figure S63).

In conclusion, surface-mediated scission of C–N bond in organometallic Pt(II) complexes on Cu(111), Ag(111), and Au(111) surfaces was studied by STM and DFT. The reactivity was found to vary greatly depending on the choice of ligands and metal substrate, Cu(111) being the most catalytic surface. For the three different Pt(II) complexes studied, their interaction strength with the metal substrate correlates with their different spatial geometries, as well as the distance of the reactive C atom from the surface. Thus, it is possible to tune the reactivity by suitable molecular design. Surface-catalyzed C–N bond cleavage, as successfully applied here, is an alternative and convenient method to produce planar Pt(II) complexes, which can otherwise be difficult to synthesize by traditional solution-processing methods.

Experimental Section

All experiments were performed in an UHV STM system (Createc) operating at a temperature of $T = 78$ K. The Au(111), Ag(111), and Cu(111) crystals were prepared by repeated cycles of Ar^+ sputtering and annealing. Synthetic procedures and characterization; supplementary STM results of **PreBr$_2$** and **C1**–**C4** complexes on Au(111), Ag(111) and Cu(111) surfaces; computational details and optimized structures are provided in the Supporting Information.

Acknowledgements

The authors acknowledge financial support from the Deutsche Forschungsgemeinschaft (TRR 61, GA 2430/1-1, DO 768/3-1, STR 1186/3-1, SFB 858). We thank Sebastian Wilde for his work on the development of complex **C1**.

Conflict of interest

The authors declare no conflict of interest.

Keywords: density functional theory calculations · Pt complexes · scanning tunnelling microscopy · surface chemistry

How to cite: *Angew. Chem. Int. Ed.* **2019**, *58*, –
Angew. Chem. **2019**, *131*, –

[1] W. Lu, B.-X. Mi, M. C. W. Chan, Z. Hui, C.-M. Che, N. Zhu, S.-T. Lee, *J. Am. Chem. Soc.* **2004**, *126*, 4958 – 4971.
[2] T. Fleetham, J. Ecton, Z. Wang, N. Bakken, J. Li, *Adv. Mater.* **2013**, *25*, 2573 – 2576.
[3] M. A. Baldo, D. F. O'Brien, Y. You, A. Shoustikov, S. Sibley, M. E. Thompson, S. R. Forrest, *Nature* **1998**, *395*, 151.
[4] D. Kim, J.-L. Brédas, *J. Am. Chem. Soc.* **2009**, *131*, 11371 – 11380.
[5] M. Mydlak, M. Mauro, F. Polo, M. Felicetti, J. Leonhardt, G. Diener, L. De Cola, C. A. Strassert, *Chem. Mater.* **2011**, *23*, 3659.
[6] C. A. Strassert, C. H. Chien, M. D. Galvez Lopez, D. Kourkoulos, D. Hertel, K. Meerholz, L. De Cola, *Angew. Chem. Int. Ed.* **2011**, *50*, 946 – 950; *Angew. Chem.* **2011**, *123*, 976 – 980.
[7] H. J. Shin, J. Jung, K. Motobayashi, S. Yanagisawa, Y. Morikawa, Y. Kim, M. Kawai, *Nat. Mater.* **2010**, *9*, 442 – 447.
[8] Y. Jiang, Q. Huan, L. Fabris, G. C. Bazan, W. Ho, *Nat. Chem.* **2013**, *5*, 36 – 41.
[9] Q. Sun, X. Yu, M. L. Bao, M. X. Liu, J. L. Pan, Z. Q. Zha, L. L. Cai, H. H. Ma, C. X. Yuan, X. H. Qiu, W. Xu, *Angew. Chem. Int. Ed.* **2018**, *57*, 4035 – 4038; *Angew. Chem.* **2018**, *130*, 4099 – 4102.
[10] J. Ren, Y. Wang, J. Zhao, S. Tan, H. Petek, *J. Am. Chem. Soc.* **2019**, *141*, 4438 – 4444.
[11] D. Y. Zhong, J. H. Franke, S. K. Podiyanachari, T. Blomker, H. M. Zhang, G. Kehr, G. Erker, H. Fuchs, L. F. Chi, *Science* **2011**, *334*, 213 – 216.
[12] R. T. Vang, K. Honkala, S. Dahl, E. K. Vestergaard, J. Schnadt, E. Laegsgaard, B. S. Clausen, J. K. Norskov, F. Besenbacher, *Nat. Mater.* **2005**, *4*, 160 – 162.
[13] H. Y. Gao, P. A. Held, M. Knor, C. Muck-Lichtenfeld, J. Neugebauer, A. Studer, H. Fuchs, *J. Am. Chem. Soc.* **2014**, *136*, 9658 – 9663.

[14] S. Wilde, D. Ma, T. Koch, A. Bakker, D. Gonzalez-Abradelo, L. Stegemann, C. G. Daniliuc, H. Fuchs, H. Gao, N. L. Doltsinis, L. Duan, C. A. Strassert, *ACS Appl. Mater. Interfaces* **2018**, *10*, 22460 – 22473.
[15] J. Ren, E. Larkin, C. Delaney, Y. Song, X. Jin, S. Amirjalayer, A. Bakker, S. Du, H. Gao, Y. Y. Zhang, S. M. Draper, H. Fuchs, *Chem. Commun.* **2018**, *54*, 9305 – 9308.
[16] B. Borca, V. Schendel, R. Petuya, I. Pentegov, T. Michnowicz, U. Kraft, H. Klauk, A. Arnau, P. Wahl, U. Schlickum, K. Kern, *ACS Nano* **2015**, *9*, 12506 – 12512.
[17] P. R. Ewen, J. Sanning, N. L. Doltsinis, M. Mauro, C. A. Strassert, D. Wegner, *Phys. Rev. Lett.* **2013**, *111*, 267401.
[18] B. Yang, H. P. Lin, K. J. Miao, P. Zhu, L. B. Liang, K. W. Sun, H. M. Zhang, J. Fan, V. Meunier, Y. Y. Li, Q. Li, L. F. Chi, *Angew. Chem. Int. Ed.* **2016**, *55*, 9881 – 9885; *Angew. Chem.* **2016**, *128*, 10035 – 10039.
[19] S. Kawai, O. Krejci, A. S. Foster, R. Pawlak, F. Xu, L. Peng, A. Orita, E. Meyer, *ACS Nano* **2018**, *12*, 8791 – 8797.
[20] D. Barton, H. Y. Gao, P. A. Held, A. Studer, H. Fuchs, N. L. Doltsinis, J. Neugebauer, *Chem. Eur. J.* **2017**, *23*, 6190 – 6197.
[21] Q. Li, B. Yang, H. Lin, N. Aghdassi, K. Miao, J. Zhang, H. Zhang, Y. Li, S. Duhm, J. Fan, L. Chi, *J. Am. Chem. Soc.* **2016**, *138*, 2809 – 2814.
[22] M. Di Giovannantonio, J. I. Urgel, U. Beser, A. V. Yakutovich, J. Wilhelm, C. A. Pignedoli, P. Ruffieux, A. Narita, K. Mullen, R. Fasel, *J. Am. Chem. Soc.* **2018**, *140*, 3532 – 3536.
[23] CCDC 1913515, 1913516 and 1913517 contain the supplementary crystallographic data for this paper. These data can be obtained free of charge from Cambridge Crystallographic Data Centre.

Manuscript received: May 20, 2019
Revised manuscript received: July 4, 2019
Accepted manuscript online: July 30, 2019
Version of record online: September 12, 2019

